45s Final CRADA Report – NFE-22-09107 Imaging Enhanced Simulation Validation for Directed Energy Deposition Additive Manufacturing

James C. Haley
Haoliang Yu
Alaa Olleak
Chong Teng
Mike Hancock
John Fortna

Unlimited Release.

June 2024

![Oak Ridge National Laboratory logo]

ORNL/TM-2024/3451

Manufacturing Science Division

IMAGING ENHANCED SIMULATION VALIDATION FOR DIRECTED ENERGY DEPOSITION ADDITIVE MANUFACTURING

James C. Haley
John Fortna
Alaa Olleak
Mike Hancock
Haoliang Yu

June 2024

CONTENTS

ABSTRACT

Directed Energy Deposition (DED) is a welding-based metal Additive Manufacturing (AM) process that relies on the programmed rastering of an electric arc or laser induced weld pool to construct a component in a layerwise fashion. The induced complex thermal field and uneven thermal contraction depends on the printed geometry and scan pattern, and as such, accumulated residual stresses and distortions are complex and difficult to predict. Several prior works have resulted in tools to combat this issue; ANSYS has developed a thermoplastic simulation package targeting DED AM, and ORNL has developed an in-situ imaging sensor package 'Stereo Correlated Optical and Pyrometric System' (SCOPS) that can spatially monitor temperature and full field strain. In this CRADA, these tools are compared in order to validate the results and complimentarily address the weaknesses in each other.

1. STATEMENT OF OBJECTIVES

The objectives of this CRADA were the following:

1-1: HPC installation and establishment of simulation pipelines
>   The Ansys workbench and mechanical software with DED AM simulation package will be installed on a CADES scalable high-performance condo, with appropriate licensing.

1-2: Deposition of three validation geometries on three DED systems
>   Three test case geometries representing different residual stress formation patterns will be designed, toolpaths generated, and deposited on three different DED systems present at the ORNL MDF, representing a heterogeneous set of design points to increase validation diversity. During deposition, a set of traditional simulation validation tools will be employed such as thermocouples and strain gauges, as well as a set of previously developed machine vision strain and temperature devices. Post-mortem characterization may include shape metrology, metallography, and neutron or x-ray diffraction residual stress measurement.

1-3: Simulation of validation geometries
>   The various geometries and machine conditions will be simulated using the installed Ansys DED Additive Manufacturing software package. Results will be spatially registered to experimental data postprocessed, and simulation methods will be iteratively refined to evaluate potential sources of error. Some of the fundamental assumptions of the simulation will be tested, including the element clustering technique and heuristics evaluated, such as appropriate element to track scaling parameters.

1-4: Phase 1 results communication
>   Data and information collected from experiments and simulation will be collated into a report and a publication as a journal article.

Further objectives were slated for Phase II of the CRADA, which was not advanced to due to both time constraints and parallel advancement of organizational capabilities which deprioritized the original technical objectives. Namely, ANSYS independently advanced the GCODE parsing capability of the DED simulation package, and ORNL has since purchased a labwide ANSYS license, enabling independent researchers direct access to HPC DED simulations, which has in effect achieved 2/3 technical objectives for Phase II. Discussion of future opportunity related to these objectives is presented in Section 6.

2. BENEFITS TO THE FUNDING DOE OFFICE'S MISSION

The Advanced Materials and Manufacturing Technologies Office (AMMTO) has an explicit commitment to accelerating adoption of innovative materials and manufacturing technologies to increase the competitiveness of a secure, domestic supply chain. Directed Energy Deposition has immense potential to support these goals in that it is capable of drastically shortening supply chains for complex components, improving performance through locally tailored material compositions and microstructures, and serving as a high-throughput alloy development platform. However, these opportunities are inhibited by the processing realities of a welding-based platform, in that accumulated residual stresses and deformation frequently cause the process to fail to produce a solid, crack-free component that meets dimensional tolerances. Improving in-situ sensing and simulation tools is a cornerstone for alleviating the process limitations of DED and expanding the capability envelope of the technology to fulfill this mission.

3. TECHNICAL DISCUSSION OF WORK PERFORMED BY ALL PARTIES

3.1 EXPERIMENTAL DESIGN

To produce a diverse set of validation data, a minimum of three geometries and three different DED systems were proposed. The performed experiments are summarized in Table 1. Schematics of the four geometries used are presented in Figure 1. The constrained wall geometry builds upon prior observation of radial deformations of thin structures with curvature due to the transferal of longitudinal thermal stresses. Stiffening pillars were added to either end of the wall to enhance this effect and help isolate it from wall end effects. A five-pass wall was used in the WAAM techniques in order to provide enough thickness for operando neutron diffraction strain mapping and was kept straight to simplify the mapping procedure. These experiments leveraged existing systems installed under lab directed research to achieve the validation aims of the CRADA without incurring time and equipment costs outside the scope of what is possible in Phase I.

Table 1. Experiments performed

Name	DED machine	DED class	Material	In-situ sensors
Constrained wall – 0°	BeAM Modulo 400	Powder laser	SS316L	TC, IR, 3D DIC, MP
Constrained wall – 90°	BeAM Modulo 400	Powder laser	SS316L	TC, IR, 3D DIC, MP
Constrained wall – 180°	BeAM Modulo 400	Powder laser	SS316L	TC, IR, 3D DIC, MP
Multipass wall	Tormach hybrid WAAM	Wire arc	Mild steel	TC, IR
3-section multipass wall	Operando neutron WAAM	Wire arc	LTT	N, TC, IR, 3D DIC

Sensor abbreviations: TC – thermocouple, IR – infrared imaging, 3D DIC – stereo Digital Image Correlation, MP – melt pool camera, N – Neutron diffraction
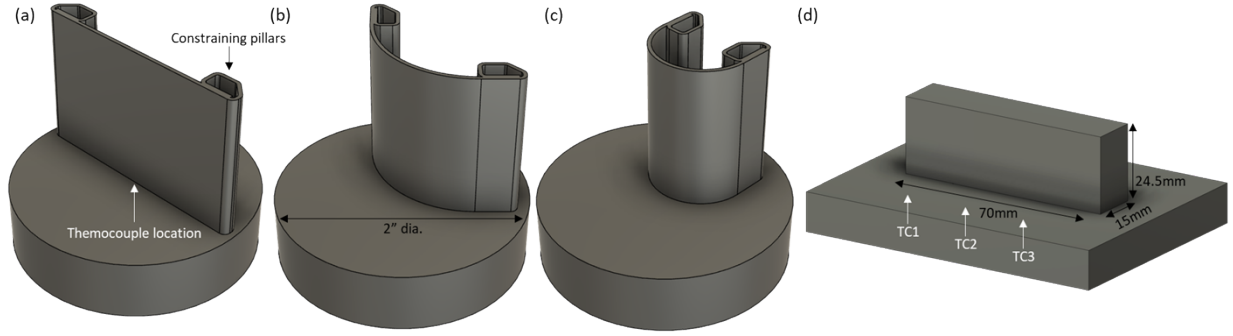
Figure 1. Four manufactured geometries designed to verify simulation performance against experimental data. (a) constrained wall 0° (b) constrained wall 90°, (c) constrained wall 180°, (d) multi-pass wall.

The three DED systems used in this work are shown in Figure 2. These systems span a diverse range of DED capabilities, from a 0.8mm bead width on the Modulo 400 laser system to the 3mm bead width typical on WAAM. Simulation was not performed on the Operando neutron system as the material used was a custom low temperature transformation (LTT) martensitic steel, which uses the martensitic expansion during phase change to alleviate the typical longitudinal tensile stresses present in DED. Simulation of this phase transition was not feasible at the time in the ANSYS DED package, but experimental results were collected for later analysis.

Figure 2. Three machines used to produce components. (a) BeAM Modulo 400, a LP-DED system, (b) a custom hybrid robotic WA-DED cell with a LE MIG welder, and (c) the OpeN-AM WA-DED cell installed at the Spallation Neutron Source for operando neutron diffraction.

3.2 IN-SITU SENSING

For each experiment performed, a range of sensors was employed to monitor either thermal or strain fields during manufacturing for comparison with simulation.

3.2.1 Thermocouples

Thin gauge type K thermocouples were either tack-welded or spot-welded with the DED system directly to substrates to provide an unambiguous thermal measurement within the domain of the simulation. Additionally, the thermocouples provide a calibration datum for infrared imaging; emissivity near the thermocouple can be directly calibrated with the thermocouple. Thermocouple readouts are presented in Figure 3. As layer times were kept consistent between constrained wall runs, substrate temperatures generally maintained replication within expected process error bounds. In the thick wall produced by

wire-arc DED, electrical crosstalk between the welder and thermocouples produced substantial readout error, which has been masked in the figure for periods where the welder was turned on.
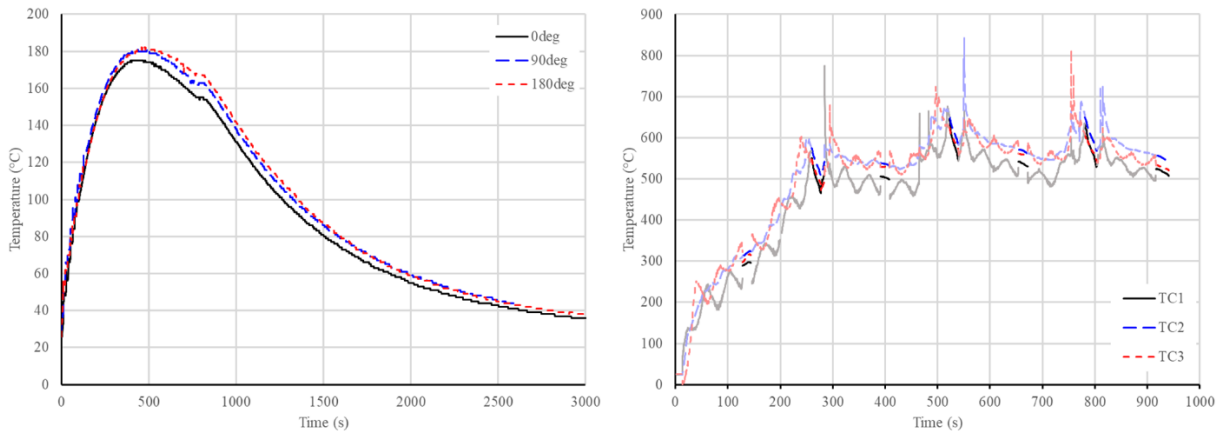

Figure 3. Thermocouple data from (a) the three constrained wall builds via LP-DED and (b) the multi-pass thick wall build via WA-DED in three locations. In (b) data is masked during printing.

In general, substrate temperature is a function the rate of heat accumulation from the component versus dissipation via conduction to fixturing, convection, and radiation. Having a thermocouple to match against simulation provides a valuable datapoint in testing the simulation values for these heat transfer mechanisms, which can have substantial impacts on the predicted component temperature and strain history.

3.2.2   Infrared Imaging

In addition to thermocouples, infrared imaging was collected for all experiments. The advantage of infrared imaging is that it collects readings spatially distributed across the surfaces of component for all times of the build. A single colorized snapshot of one experiment and four example picked points are plotted in Figure 4. These results are compared with simulation in Section 3.3.

One disadvantage to infrared imaging is its calibration sensitivity to emissivity, which is a function of material, surface roughness, oxidation, and temperature. As these conditions can vary spatially over the build as well as in time, static methods for correcting for these effects will suffer inaccuracies. In this experiment, for simplicity a reading from the thermocouple near the base of the wall was considered ground truth for the infrared intensity response function, and emissivity was estimated by comparing pixels at the bottom of the wall with the substrate at a known temperature.
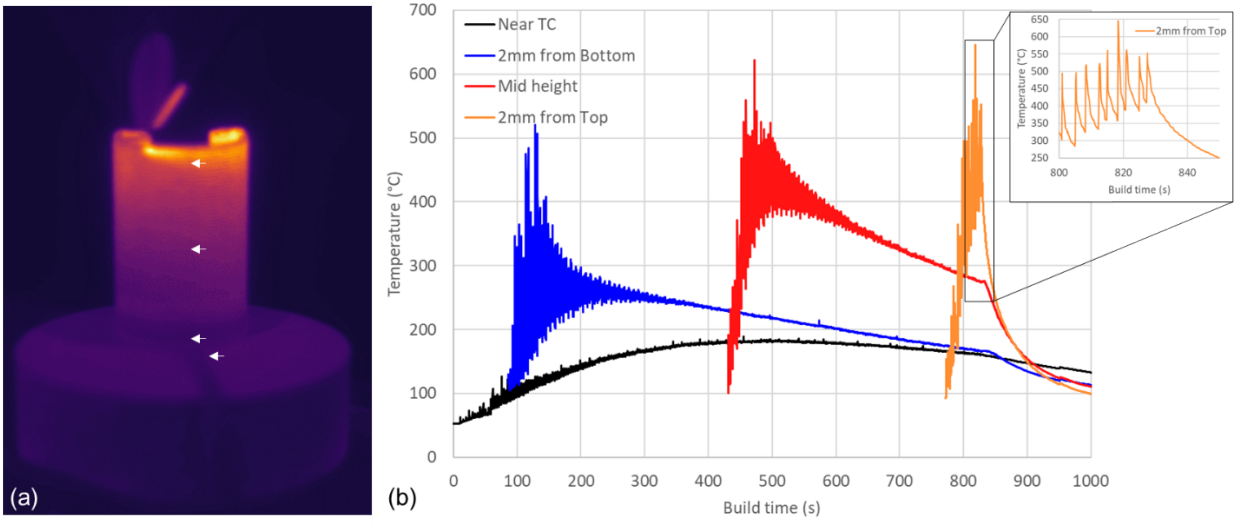
Figure 4. Infrared data for the 180° constrained wall, plotted (a) spatially and (b) over time for points indicated.

3.2.3   Stereo Digital Image Correlation

Using a pair of high-resolution of monochromatic visible light cameras, stereo Digital Image Correlation (DIC) was performed on the three constrained wall experiments to measure extrinsic component strain over the course of deposition. DIC requires a reference state to calculate deformation, which in this case was set to the final cold state of the wall. Using triangulation from both cameras, surface strains are measured in 3D, allowing for calculation of deformation out of the plane of the wall geometry, as depicted in Figure 5, for the time between the last deposition pass and the cold state. This form of deformation is particularly deleterious to dimensional accuracy as it misaligns the wall from the next layer of deposition.
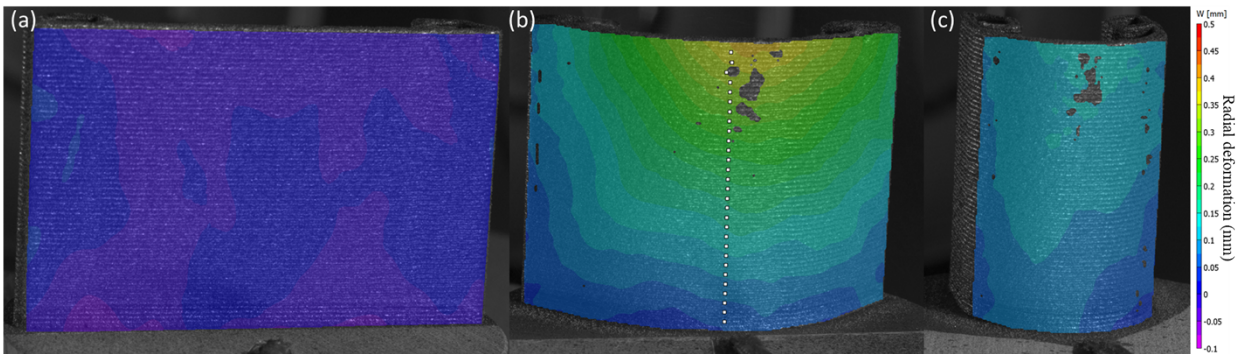

Figure 5. Stereo Digital Image Correlation (DIC) results plotting radial deformation between the final cold state and just after the final layer was printed, for (a) 0°, (b) 90°, and (c) 180° constrained wall geometries.

Several features of note were observed from DIC. First, the geometry with a middling radius of curvature displayed the highest out of plane deformation. This can be attributed to the longitudinal stresses being relieved through radial deformation, which must be of a larger magnitude for mild curvatures to achieve

the same relief. The flat wall, in contrast, cannot alleviate longitudinal stresses this way, and displays little out of plane deformation. The magnitude of deformation was observed to be on the order of 0.5mm, which is compared to simulation and discussed in Section 3.3.

3.3   SIMULATION

Four thermoelastic simulations of the experimental geometries were performed using the ANSYS DED simulation package, as overviewed in **Figure 6**.
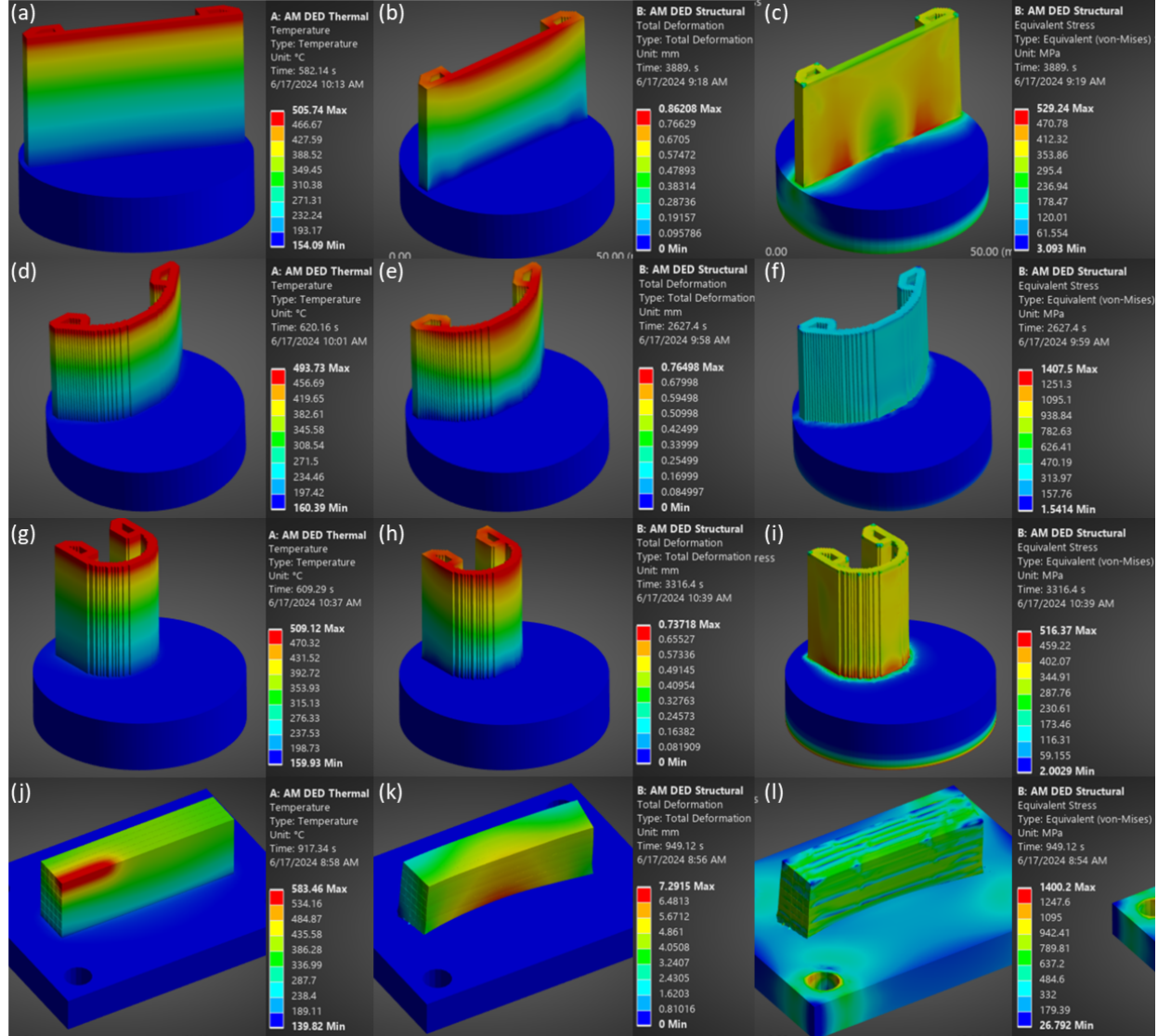

Figure 6. Overview of ANSYS DED simulation results for the four experimental geometries. Left panels (a,d,g,j) displaying the temperature just after the final deposition pass, center (b,e,h,k) showing the total deformation between deposition location and the final cold state, and right (c,f,i,l) showing von-Mises stress.

The DED package incorporates element activation by parsing printer GCODE directly, which activates element clusters that follow the rastering of the heat source. This is a necessary improvement for DED over prior LPBF focused simulation, which activated entire layers simultaneously to improve calculation time. As DED frequently accumulates more local heat due to a larger melt pool, the layer-wise

assumption breaks down and provides inferior accuracy. The local heating effects due to the final track's element cluster can be observed in Figure 6(g).

All FEA simulations are bounded by the accuracy of the constituent assumptions. Comparison to experimental data allows us to assess their accuracy, with multiple data forms providing better deconvolution of effects. First, substrate thermocouple data is a good bundle estimate of the accuracy of the overall heat transfer rates. As can be seen in Figure 7, the temperature for the constrained wall simulation near the bottom of the build comes close to matching the values from the thermocouples (Figure 3) at the end of the build, but tends to rise over time asymptotically to the end of the build instead of dropping linearly as the build progresses away from the substrate as observed by the blue line in Figure 4. This tends to imply that further tuning of convection coefficients and heat input are required; the expectation is that as the active deposition area leaves the proximity of the substrate, heat transfer to the substrate becomes slower and convection/radiation off of the wall sides becomes significant. In 7b, the simulated thermocouple temperatures are substantially lower than the observed data, implying that the process imparts more heat than assumed to the newly deposited material, requiring further tuning.
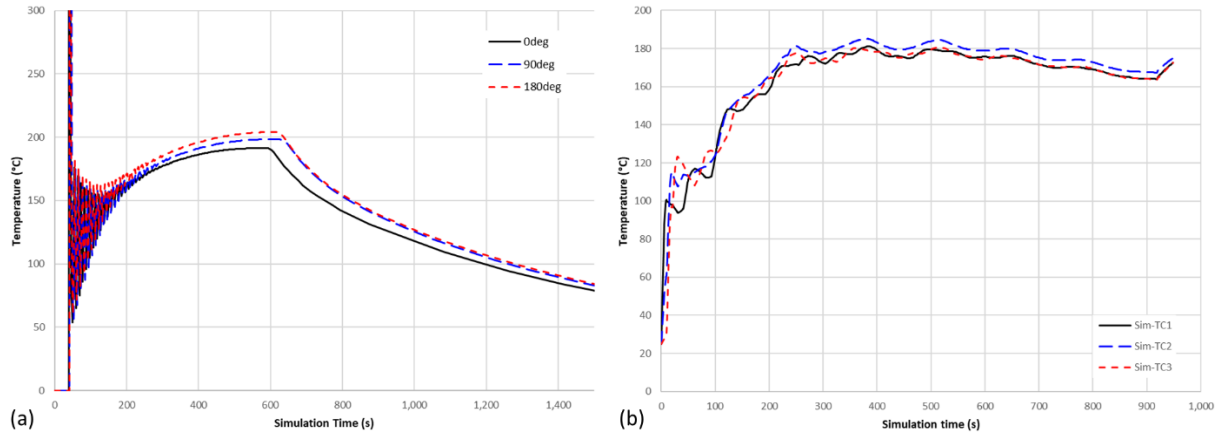

Figure 7. Simulated temperature readouts from (a) 2mm above substrate on constrained walls, and (b) three thermocouple locations on the thick multi-pass wall.

Data from DIC presented in Figure 5 for the constrained wall shows a similar distribution and magnitude of deformation, with a few notable differences. First, the simulated deformations are totaled between the point of solidification (element activation) and the cold state of the part, unlike in the displayed DIC results which are from the last layer to the cold state. As substantial deformation can occur during the printing, it is expected that the simulated deformation would be higher. Second, the deformation shown in Figure 6 includes the deformation in the build direction, which is expected to contract substantially as it is not firmly constrained, leading to higher total deformation on the 0deg flat wall than was observed in the out-of-plane component in DIC. For the walls with curvature, Von-Mises stress shows that there is a mostly even distribution along the build direction, with some stress concentration near the substrate where x/y plane deformations are constrained and have sharp corners. An interesting effect was seen in the Von-Mises stress of the flat wall in Figure 6(c), where the constraining pillars appear to have redistributed some of the stress normally found on the bottom corners of thin walls toward the center into two 'hot spots'.

4.   SUBJECT INVENTIONS

No subject inventions were generated as a part of this CRADA.

5.   COMMERCIALIZATION POSSIBILITIES

The work performed under this CRADA has underscored some of the issues in the routine calibration of achieving quantitatively predictive simulation of DED, which introduces the possibility of several commercial tools that may accelerate the process. First, on the experimental end, extraction and alignment of data to the same frame used in simulation is a manual and laborious process. A software tool or workflow to automate the extraction and alignment procedure would reduce the overhead involved in collecting more data for validation. Second, parameter tuning in a simulation to match reality can also be a labor-intensive process. Several generic tools that help exist in ANSYS, such as the workbench and parameter optimization kits, but a DED focused simulation 'autotune' that uses some of the process knowledge to target optimization of less certain parameters first may decrease time required to obtain an accurate model parameter set.

6.   PLANS FOR FUTURE COLLABORATION

Going forward, collaboration is possible in several ways. First, ORNL has purchased a lab-wide license to the ANSYS suite, so the used DED simulation tools will be available to all researchers for any project that requires it. Having an established workflow and user base allows the organization to develop the expertise in the software usage and greatly expands the utility reaped. As projects use this simulation for various studies, technical support from the ANSYS development team may be beneficial in establishing new features to enhance the functionality of the software in the context of 5-axis deposition, advanced materials with thermal and stress induced property responses, and hybrid manufacturing.

7.   CONCLUSIONS

In Phase I of this CRADA, in-situ sensor data from five experimental geometries across three machines and two distinct classes of DED technology were collated for simulation validation. Simulation was performed for the four geometries with supported material data sets in ANSYS, and results exported for comparison against in-situ data. Results showed viability for using the ANSYS DED element cluster activation method for realistic thermoplastic simulation that resolves the scan strategy effects. This study highlights the importance of a simulation calibration workflow that incorporates in-situ time-domain data for DED and has supported the lab wide licensing of ANSYS tools for ongoing Additive Manufacturing research.

Final Report Certification
for
CRADA Number _____ **NFE-22-09107** _____

Between

UT-Battelle, LLC

and

ANSYS, Inc.
_____
(Participant)

The following certification is made for the subject final report:

1. (a) ☐ The final report contains information that qualifies as "Protected CRADA
Information" (PCI). The PCI legend is printed on the report cover, and
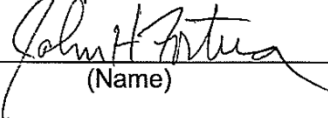the PCI is clearly identified.

OR

(b) ☒ The final report does not contain "Protected CRADA Information." The
"Approved for Public Release" legend is printed on the report cover.

2. The final report does not contain Proprietary Information.

3. By the signature below, the Participant has no objection to the public
distribution of the final report due to patentable information.

For the Participant:

_____
(Name)

Senior Director of R&D
_____
(Title)

07/01/2024
_____
(Date)

ORNL-851 (9/2007)